



# Determination of thermal effects accompanying the austempering of copper–nickel ductile iron

A. Gazda\*

Center of High Temperature Studies, Foundry Research Institute, 73 Zakopianska St., 30-418 Krakow, Poland

## ARTICLE INFO

### Article history:

Received 16 September 2009

Received in revised form

24 November 2009

Accepted 26 November 2009

Available online 3 December 2009

### Keywords:

Austempered ductile iron (ADI)

Isothermal calorimetry

DSC

Enthalpy change

## ABSTRACT

Using especially designed and constructed isothermal calorimeter, the austempering of Cu–Ni ductile iron was carried out at temperatures of  $T_{pi} = 270, 350, 390$  and  $430$  °C, simultaneously with the measurement of accompanying thermal effects. The values of enthalpy changes  $\Delta H$  show the correct and expected trend, varying from  $45$  J/g at  $T_{pi} = 430$  °C to  $70$  J/g at  $T_{pi} = 270$  °C.

The changes of enthalpy were observed to increase with decreasing temperature of the isothermal transformation during austempering. The results of the present work did not allow revealing the influence of alloying elements, i.e. Cu and Ni, on the heat of isothermal transformation.

The discrepancies between the results of the actual measurements and the results quoted in other papers were discussed in terms of DSC measurements.

© 2009 Elsevier B.V. All rights reserved.

## 1. Introduction

The structure and the resulting mechanical properties of austempered ductile iron depend on the mechanism and kinetics of phase transformations proceeding successively during quenching followed by isothermal transformation:

1.  $\gamma(C_0) \rightarrow \alpha + \gamma_s$  (C) (ausferrite forming).
2. Stability of structure  $\alpha + \gamma_s$  (C) (processing window).
3.  $\gamma_s(C) \rightarrow \alpha + Fe_3C$  (or  $\epsilon$  carbide) (carbides precipitation).

At the end of the 1st stage, ausferrite with maximum amount of fine acicular ferrite  $\alpha$  and reacted stable carbon-saturated austenite  $\gamma_s$  (C) is forming. The beginning of the 3rd stage corresponds to the start of carbides precipitation from austenite and decomposition of ausferritic matrix. The heat treatment processing window (2nd step) is an optimum stage for ausferrite stabilization.

The temperature of isothermal transformation affects its kinetics and the cast iron microstructure; with decreasing temperature the ferrite plates become smaller, giving rise to increased strength and hardness.

The complex isothermal transformation generates energy changes and can be investigated by means of a calorimetric method, which enables quantitative analysis of the mechanism and kinetics of phase transformations.

There are several papers devoted to measurements of the thermal effects of ausferrite formation, mainly based on the Derivative Thermal Analysis method [1–3] applied to determine the transformation kinetics and heat treatment parameters.

From the thermodynamic point of view, phase transition resulting in ausferrite formation consists of the three elementary reactions giving at  $\sim 500$  °C the total thermal effect of  $\Delta H = -8.2$  kJ/mol [4]. These are the following reactions:

- exothermic:  $Fe_\gamma \rightarrow Fe_\alpha$  in pure iron ( $\Delta H = -6.9$  kJ/mol);
- exothermic: precipitation of carbon from austenite ( $\Delta H = -3.5$  kJ/mol);
- endothermic: formation of cementite ( $\Delta H = +2.2$  kJ/mol).

Depending on the transformation temperature and high-carbon austenite volume fraction, the enthalpy values of  $20$ – $40$  J/g were calculated. This evaluation does not take into account the contributions of the energy of the austenite/ferrite interface formation and stress energy.

The new isothermal ADI calorimeter based on DTA (Differential Thermal Analysis) principle and operating in an isothermal “drop in” mode described in details in [5] enables manufacturing ADI in laboratory scale with simultaneous recording of the thermal effects of phase transformations proceeding during austempering. The calibration of the device equipped with a K type thermocouple sensor guarantees the required measurement sensitivity and uncertainty at a level of 5%.

\* Tel.: +48 12 2618515; fax: +48 12 2660870.

E-mail address: [agazda@iod.krakow.pl](mailto:agazda@iod.krakow.pl).

**Table 1**  
Chemical composition of the base ductile iron in wt%.

Alloy	C	Si	Mn	Mg	Cu	Ni
A0	3.70	2.30	0.10	0.080	0.55	–
A1	3.50	2.55	0.08	0.065	0.50	0.97
A2	3.50	2.57	0.08	0.085	0.50	1.43
B0	3.80	2.30	0.18	0.080	0.93	–
B1	3.50	2.70	0.20	0.075	0.93	0.90
B2	3.70	2.50	0.08	0.090	0.90	1.37

## 2. Preparation of materials

The melts of base ductile iron without molybdenum were performed and two groups of alloys with different Cu (designated A,B) and Ni (designated 0,1,2) contents were prepared. Table 1 shows chemical composition of the investigated materials. The typical as-cast ductile iron microstructure is shown in Fig. 1a and b.

Determined by a dilatometric method, the values of  $A_{C3}$  temperature were found to be in the range of 870–880 °C, and so the austenitizing temperature of  $T_a = 900$  °C and the time of austenitizing  $t_a = 60$  min were accepted for all the alloys under investigation.

## 3. Calorimetric measurements in isothermal conditions

The samples prepared for measurements in isothermal calorimeter [5] had fixed dimensions of  $\Phi 3.5$  mm  $\times$  3 mm. Calorimetric measurements were carried out according to the adopted procedure of ADI manufacture. The ductile iron samples were austenitized at 900 °C for 60 min in an austenitization furnace followed by drop into a transient cooling chamber to quickly reach the temperature of austempering ( $T_{pi}$ ). Adjacent to the chamber, a water cooler and an inert gas cooler enabled quick cooling down

**Table 2**  
Optimum parameters of ductile iron heat treatment in isothermal calorimeter.

$T_{pi}$ (°C)	$T_{pi}$ (min)	$\tau_o$ (s)	$q$ (K/s)
270	120	27	23.3
350	90	20	27.5
390	45	17	30.0
430	30	15	31.3

of the sample. Finally, using simple manipulator, the sample was dropped into the calorimeter crucible placed inside the calorimeter sensor.

At a constant austempering temperature, the holding time  $\tau$  of the sample in a transient chamber depends only on the sample temperature  $T_s$  and as such has been established experimentally (Table 2). Minimalization of specific thermal effects ( $C_p \Delta T$ ), arising as a result of temperature difference  $|T_s - T_{pi}|$  which should approach zero, was the criterion for optimum cooling time choice  $\tau = \tau_o$ . This simplified approach was successful because the samples of an identical geometry and similar thermal properties were heat treated in the calorimeter characterized by stable and reproducible conditions. Additionally, two measurements were taken for each alloy at different but very close cooling rates  $q$  to produce two different thermal effects: endothermic if  $\tau > \tau_o$  ( $T_s < T_{pi}$ ) and exothermic if  $\tau < \tau_o$  ( $T_s > T_{pi}$ ).

The data from [1] and the metallographic examinations prove that the applied cooling rates have been sufficient to produce the correct ADI structures (Fig. 2a and b).

Figs. 3 and 4 show calorimetric curves (upper part of diagram) for optimum conditions of isothermal transformation (processing window). Depending on the sign of the expression  $|T_{pi} - T_s|$ , either endothermic (heating of “colder” sample up in the calorimeter crucible) or exothermic (cooling of “warmer” sample in the calorimeter crucible) effects occur.

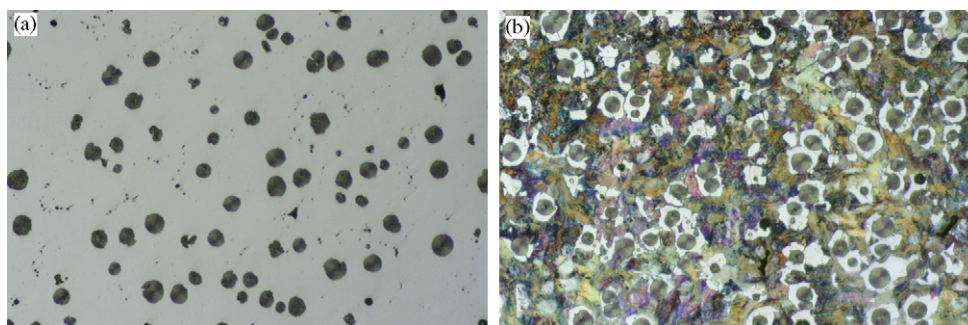


**Fig. 1.** Microstructure of alloy A0; magnification 100 $\times$ , (a) metallographic cross-section after polishing; (b) metallographic cross-section after etching.

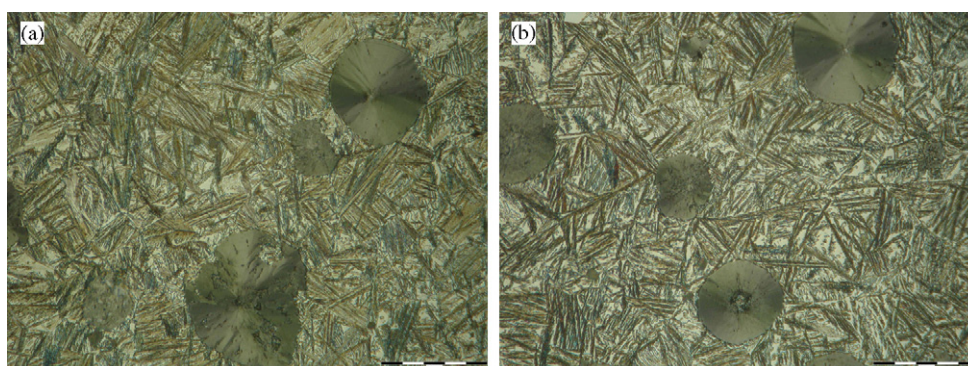


**Fig. 2.** Microstructure of alloys after heat treatment at 350 °C for 60 min in isothermal calorimeter; magnification 500 $\times$ , metallographic cross-section etched with HNO<sub>3</sub> (a) alloy A0; (b) alloy A2.

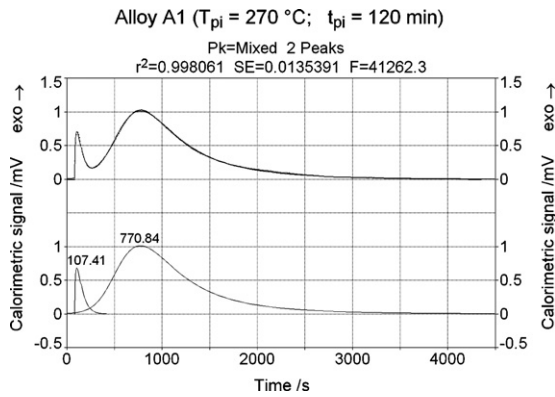


Fig. 3. The calorimetric curves - as obtained in experiments and after deconvolution of complex peak; alloy A1,  $T_{pi} = 270\text{ }^{\circ}\text{C}$  ( $T_s > T_{pi}$ ).

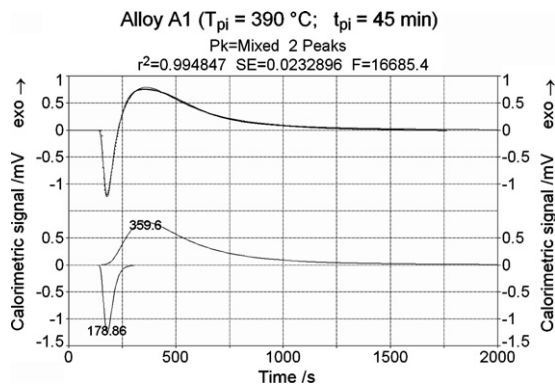


Fig. 4. The calorimetric curves - as obtained in experiments and after deconvolution of complex peak; alloy A1,  $T_{pi} = 390\text{ }^{\circ}\text{C}$  ( $T_s < T_{pi}$ ).

Consequently, the exothermic effect connected with the 1st stage of transformation has appeared (see example: upper part of diagram in Figs. 3 and 4). The endothermic effect related to carbon dissolution in austenite was not observed because of a slow kinetics of this process. To eliminate the missing thermostructural effects, the deconvolution of complex peaks was done by means of PeakFit v.4.12 software (see example: lower part of diagram in Figs. 3 and 4).

Fig. 5a and b presents a summary of the calorimetric investigations performed for two series of the ductile iron with different copper content levels.

The values of the thermal effects connected with austenite decomposition under isothermal conditions are comprised in a

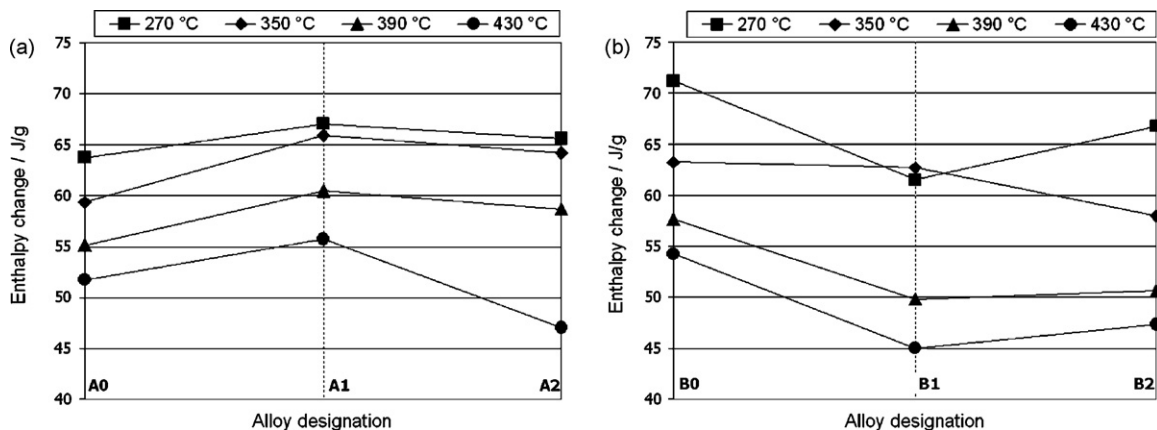


Fig. 5. Comparison of results obtained in the isothermal calorimeter, (a) alloys group A; (b) alloys group B.

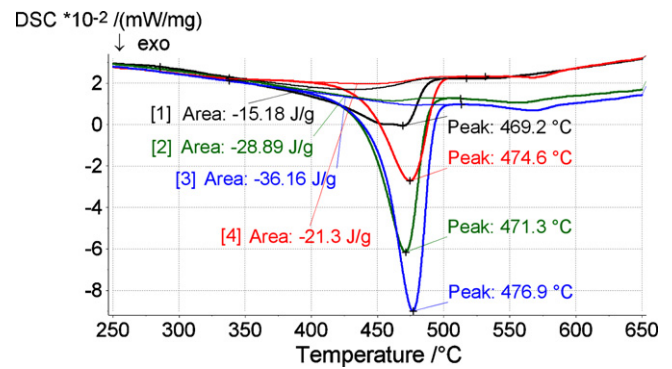


Fig. 6. DSC curves plotted for alloy A0 subjected to heat treatment in the isothermal ADI calorimeter: [1]  $T_{pi} = 270\text{ }^{\circ}\text{C}$ , [2]  $T_{pi} = 350\text{ }^{\circ}\text{C}$ , [3]  $T_{pi} = 390\text{ }^{\circ}\text{C}$  and [4]  $T_{pi} = 430\text{ }^{\circ}\text{C}$ .

range from 45 J/g (at  $T_{pi} = 430\text{ }^{\circ}\text{C}$ ) to 70 J/g (at  $T_{pi} = 270\text{ }^{\circ}\text{C}$ ). The calculated values of the heat of transformation differ from the results obtained by the method of Derivative Thermal Analysis [1,2] regarding both temperature values and temperature trends but are close to those obtained in [3].

On the other hand, the thermodynamic data computed by means of JMatPro software and checked experimentally for steels [6] as well as the results cited in [7] indicate the values of about 80 J/g, confirming the results obtained in the present work.

Additional investigations were performed by differential scanning calorimetry (DSC) to explain some divergencies in the thermodynamic data on ausferrite transformation obtained in the present work and in literature.

#### 4. DSC measurements

The ADI grades were manufactured in the isothermal ADI calorimeter under optimum heat treatment conditions of the processing window (Table 2) at temperatures of  $T_{pi} = 270\text{ }^{\circ}\text{C}$ ,  $350\text{ }^{\circ}\text{C}$ ,  $390\text{ }^{\circ}\text{C}$  and  $430\text{ }^{\circ}\text{C}$ .

ADI samples were heated at a rate of 5 K/min in argon protective atmosphere in Netzsch DSC 404C and thermal curves were recorded. To establish correct baseline, the method of double DSC runs was performed under the same conditions. The first DSC curve reflects the situation when the ausferrite structure decomposition takes place; the second run is performed on sample after the decomposition of ausferrite. The difference, nearly independent of thermophysical properties of the material, shows a nonreversible process of the decomposition of ausferrite during slow heating of ADI sample.

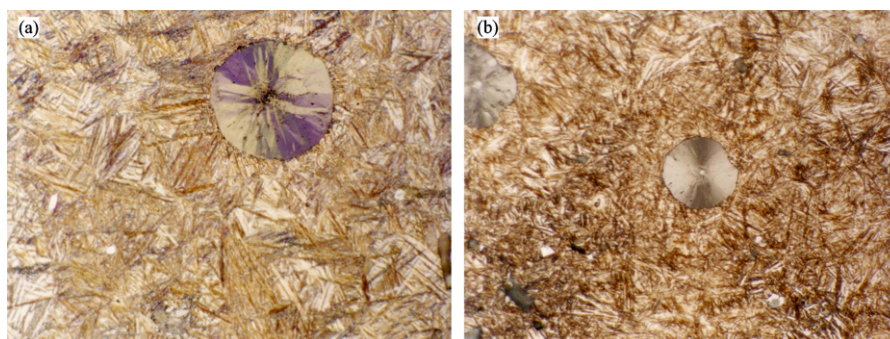


Fig. 7. Microstructure of alloy B2 (270 °C/120 min); magnification 500×; (a)  $T_{\text{temp}} = 420$  °C; (b)  $T_{\text{temp}} = 530$  °C.

The exemplary DSC curves plotted for several ADI grades obtained from base alloy A0 are visible in Fig. 6.

The DSC curves are complex in the whole range of the heating temperatures up to a point of the eutectoid transformation but distinct exothermic effects (400–500 °C) reflect the processes of ausferrite decomposition. The surface area of the DSC peaks ( $\Delta H$ ) and the temperature of their maxima increase with the increasing temperature of isothermal transformation. It proves that the amount of high-carbon austenite and carbon content increases in this phase. Then the peaks become narrower and their shapes less complex, thus proving the disappearance of low-carbon austenite. The only exception are alloys after heat treatment at the highest austempering temperature, i.e.  $T_{\text{pi}} = 430$  °C; the narrow processing window causes the formation of low-carbon austenite and martensite.

For all the alloys under investigation, the thermal effects calculated from the DSC measurements for an inverse transformation are in the range of 15–36 J/g, which is consistent with the results obtained in [4,8,9] and with theoretical considerations.

The conclusion is that the results of austempering simulation obtained in isothermal ADI calorimeter are higher than those obtained for inverse transformation (decomposition of ausferrite) by means of the DSC method. A probable explanation of this fact is to be sought in the following statement: the isothermal *in situ* calorimetric measurements of thermal effects allow for the contribution of surface (interfacial) energy necessary for the creation of interphase boundary and stress relaxation. The total enthalpy change  $\Delta H$  accompanying the transformation equals to:

$$\Delta H = \Delta H^{\circ} + \Delta H^{\text{s}}; \quad \Delta H^{\text{s}} = \Delta H^{\sigma} \cdot \Delta A = \Delta H^{\sigma} \cdot A \quad (1)$$

where  $\Delta H^{\circ}$  means bulk enthalpy change and  $\Delta H^{\text{s}}$  is the surface enthalpy fraction.  $\Delta H^{\sigma}$  denotes the specific surface enthalpy change, accompanying the formation of interphase specific area  $A$  and the relation  $\Delta H^{\sigma} = \partial \Delta H / \partial A$  suggests the way in which this quantity can be experimentally determined in future by means of calorimetric measurements and quantitative metallographic observations.

The contribution of surface enthalpy was not recorded in DSC runs during slow heating of 5 K/min; the microstructural examinations (Fig. 7a and b) have shown that at a relatively high overheating (tempering) temperature of  $T_{\text{temp}} = 530$  °C, the structure of acicular ferrite is still present.

Decomposition of ausferrite during DSC measurement proceeds mainly by means of precipitation of carbon from high-carbon reacted stable austenite.

To what degree taking into account the surface enthalpy contribution can explain the observed discrepancies should be the aim of future investigations; in the case of eutectoid

austenite → pearlite transformation proceeding at relatively high temperature, the value of specific surface energy  $\Delta G^{\sigma} = 0.94$  J/m<sup>2</sup> and enthalpy change of that contribution amounts to several J/g [10,11].

The measurements taken in the isothermal ADI calorimeter were compared and explained with the aid of differential scanning calorimetry, thus proving usefulness of the new laboratory method.

The value of the thermal effect connected with austenite decomposition under isothermal conditions is a resultant of complex effects: exothermic, of fine acicular ferrite forming and endothermic, of reacted stable carbon-rich austenite developing which can be separately investigated as inverse transformation by means of DSC.

The complementary application of DSC and new isothermal ADI calorimeter comprise convenient and fast tool for stability of ausferrite structure determination and ADI heat treatment parameters designing.

## 5. Conclusions

The carried out investigations allow the following conclusions to be formulated:

- the austempering heat treatment of Cu–Ni ductile iron at temperatures of 270, 350, 390 and 430 °C has been performed with simultaneous recording of exothermic thermal effects accompanying the formation of austempered ductile iron ADI;
- the values of enthalpy changes  $\Delta H$  during austenite → acicular ferrite + reacted stable carbon-saturated austenite transformation are comprised in a range from 45 J/g ( $T_{\text{pi}} = 430$  °C) to 70 J/g at  $T_{\text{pi}} = 270$  °C;
- the values of the thermal effects show correct tendency because at low temperatures of the isothermal transformation the content of the acicular ferrite with small dimensions and large interphase surface demanding much more extra surface energy is higher than at high isothermal transformation temperatures; at higher temperatures the carbon dissolution in austenite occurs, reducing additionally the global thermal effect;
- the results of the present work are insufficient to estimate the effect of alloying elements, i.e. of Cu and Ni, on the heat of isothermal transformation;
- the values of enthalpy changes determined by means of isothermal ADI calorimeter are not in good agreement with the results obtained by the method of Derivative Thermal Analysis but approximate the thermodynamic data [8,9];
- the values of enthalpy changes during inverse transformation determined by means of DSC are in good agreement with the results of other works utilizing DSC technique [4,8,9] and with the theoretical evaluation;

- thermal effects recorded in the isothermal calorimeter allow for the contribution of surface energy, necessary for the interphase surface formation and relaxation energy. These effects were not recorded in DSC measurements because the structure of acicular ferrite has survived up to a relatively high temperature of tempering in DSC apparatus and that is the reason of a discrepancy observed between the two applied methods of thermal analysis;
- the measurements taken in the isothermal ADI calorimeter were compared, verified and explained with the aid of differential scanning calorimetry, thus proving full applicability of the new laboratory technique to ADI investigation and its compatibility with DSC method.

### Acknowledgement

This work was financially supported by Polish Committee of Scientific Research (KBN); grant No. 4 TO8B 031 entitled: "Investigation of thermal stability and optimization of heat treatment parameters of Cu–Ni ADI by means of thermal analysis method".

### References

- [1] C.H. Chang, T.S. Shih, *Trans. Jpn. Foundrymen's Soc.* 13 (1994) 56–63.
- [2] W. Kapturkiewicz, E. Fraś, J. Lelito, A. Burelko, *Mater. Sci. Forum* 508 (2006) 585–590.
- [3] T.S. Shih, S.Y. Chau, C.H. Chang, *AFS Trans.* 104 (1996) 557–564.
- [4] M. Baricco, G. Franzosi, R. Nada, L. Battezzati, *Mater. Sci. Technol. (UK)* 15 (1999) 643–646.
- [5] A. Gazda, *Odlewnictwo–Nauka i Praktyka* 1–2 (2007) 14–24.
- [6] N. Saunders, Z. Guo, A.P. Miodownik, J.P. Schillé, 22nd CAD-FEM Users' Meeting 2004 International Congress on FEM Technology with ANSYS CFX & ICEM CFD Conference, November 10–12, Dresden Germany, 2004.
- [7] J.-M. Bergheau, P. Duranton, H. Porzner, F. Boitout, Coupled carbon diffusion, metallurgical transformation and heat Transfer models applied to the as-hardening process, in: *Proc. of EUROPAM 2000, 10th Int Conference and Exhibition on Virtual Prototyping by Numerical Simulation*, Nantes, France, 2000.
- [8] H. Bayati, R. Elliott, 20th ASM Heat Treating Society Conference Proceedings, St. Louis, MO, ASM International, 9–12 October 2000, 2000, pp. 593–601.
- [9] A. Gazda, *Acta Met. Slovaca* 7 (2001) 74–79.
- [10] J.J. Kramer, G.M. Pound, R.F. Mehl, *Acta Met.* 6 (1958) 763.
- [11] S.E. Offerman, L.J.G.W. van Wilderen, N.H. van Dijk, J. Stietsma, M.Th. Rekveldt, S. van der Zwaag, *Acta Mater.* 51 (2003) 3927–3938.